2014 IEEE International Conference on Robotics & Automation (ICRA)
Hong Kong Convention and Exhibition Center
May 31 - June 7, 2014. Hong Kong, China

Experimental Friction Identification in Robot Drives

Joerg Baur, Sebastian Dendorfer, Julian Pfaff, Christoph Schütz, Thomas Buschmann and Heinz Ulbrich

Abstract— **The drive mechanism of many robot joints are composed of an electrical actuator and a gear transmission. Besides actuator dynamics and gear elasticity, friction effects are of particular importance for accurate dynamic modeling. This paper presents the design and development of a modular testbed for experimental friction identification in modular robot drives. We have used this testbed to investigate modules that were developed at our institute for the humanoid robot Lola and an agricultural manipulator. We discovered that a friction law, similar to a law proposed in the literature, can be very accurately fitted to our measurements.**

I. INTRODUCTION

The development of robot manipulators could hardly be achieved without a dynamic simulation model to design the electrical components and mechanical parts. The more accurate the model, the more beneficial it can be for the system design and realization of efficient control concepts. For robotic manipulators, one common approach for the design of a joint drive mechanism is the combination of electrical actuators with high gear ratio transmissions. These gears usually have a high amount of friction which must be taken into account at the design stage and incorporated into the dynamic model. Given the difficulty of modeling friction effects, usually the design engineer has to rely on specifications provided by the gear manufacturer. Nevertheless, under conservative assumptions, it is possible to successfully design the system components. However, to further improve the dynamic model and to evaluate the system design, identifictaion on the real system is necessary. In this study, the design of a testbed to experimentally investigate friction effects in robotic drive modules is presented. Measurements on modules, developed for the humanoid robot Lola as well as measurements on a test joint, recently designed for an agricultural manipulator (cf. Fig. 1) as part of the EU-project CROPS, were conducted. This is easily possible since both robots are designed out of integrated drive modules and assembled at our institute. The paper is organized as follows. In the next section, we give a short overview of related work concerning friction identification, focusing particularly on modeling HarmonicDrive gears. In Section III the set-up and dynamic modeling of the drive modules is addressed. Section IV describes the requirements, the design of the testbed and the test procedure for the experimental friction identification. The results are presented in Section V and a short conclusion is given in the end.

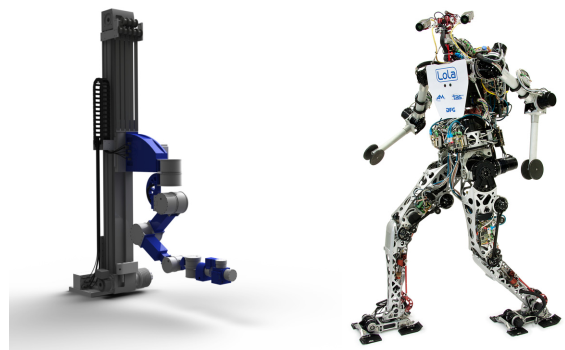

(a) Manipulator Prototype (CAD) (b) Humanoid Robot Lola

Fig. 1: Robots at the Institute of Applied Mechanics

II. RELATED WORK

In the last decades, many researchers have worked on the modeling and experimental identification of friction phenomena in machinery. Nevertheless, according to [1], system modeling, in particular modeling of friction effects, solely based on catalog data will not lead to an accurate dynamic model. An apparatus for experimental friction measurements in bearings [2], [3] as well as various experimental set-ups for parameter identification in HarmonicDrive gears are reported in the literature. For friction identification in HarmonicDrive gears it is common to fit model parameter to measurements. A basic experimental setup is composed of an electrical actuator, driving the input side of the gear with the possibility to fixate the output shaft [1], [4]. In the work of [5], [6], a testbed was designed with an inertia load on the output side of the gear for unrestrained motion experiments. Note that it is impossible with this set-up to represent arbitrary load cases. Sometimes it is not easily possible to investigate individual drive units of a robot (e.g. when buying an industrial manipulator), in which case a parameter identification must directly performed on the system as a whole [7], [8]. The major friction loss in HarmonicDrive gears occurs in the tooth-meshing of the circular and flexspline. Other effects comprise viscous damping of the wave generator and flexspline bearings, as well as structural damping of the flexspline [6]. More detailed models consider position dependent friction and influences of resonance vibration, due to higher torques in the meshing [1]. A very detailed description of HarmonicDrive gear modeling and experimental parameter identification is given in [9].

This research was partly funded by the European Commission in the 7th Framework Programme (CROPS GA no 246252).

The authors are with the Institute of Applied Mechanics, Technische Universität München, Boltzmannstr. 15, 85748 Garching, Germany {j.baur, s.dendorfer, julianpfaff, christoph.schuetz, thomas.buschmann, ulbrich}@tum.de

III. MODELING AND SIMULATION

For the mechatronic design of a robot, it is important to derive a dynamic model of the system. The model should reflect the major physical effects, while being as simple as possible. For a modular agricultural manipulator, we are currently developing integrated drive modules at different scales. Each module contains the following main components:

- Frameless brushless DC (BLDC) Motor
- HarmonicDrive Gear Transmission
- Motor Controller
- Incremental Encoder (on motor shaft)
- Absolute Encoder (on output shaft)
- Data and Power Interface on Input and Output side

To describe the dynamics of the module, a lumped component model of relevant mechanic elements is given in Fig. 2, with the motor and gear rotational inertia J_m, the motor velocity $\dot{\varphi}$ and the actuator torque T_a acting on the intertia. The friction loss in the bearings of the motor shaft is added to the gear's friction. The HarmonicDrive gear is described with a nonlinear friction term T_f, the transmission ratio N and a (nonlinear) stiffness c_{fs} and damping b_{fs} on the gear's output side. The load position and velocity is described by q and $\dot{q}$ and it has the inertia J_l where the torque T_l is applied. Using

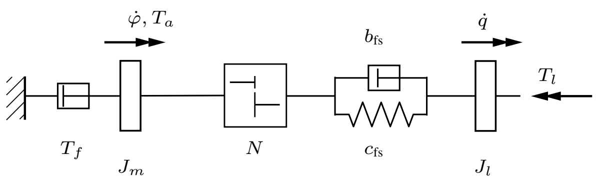

Fig. 2: Schematic diagram of the module mechanics

the Angular Momentum Theorem, the equations of motion for the system are given by

$$\ddot{\varphi} = \frac{1}{J_m}\left(T_a + T_g\right) \tag{1}$$

$$\ddot{q} = \frac{1}{J_l}\left(-T_l - T_s - T_b\right) \tag{2}$$

$$T_g = T_f + \frac{1}{N}\left(T_s + T_b\right) \tag{3}$$

with the torque T_g from the gear input side. The elasticity and damping torques T_s and T_b of the gear can be modeled as follows

$$T_s = \left(q - \frac{\varphi}{N}\right) c_{\text{fs}} \tag{4}$$

$$T_b = \left(\dot{q} - \frac{\dot{\varphi}}{N}\right) b_{\text{fs}} \tag{5}$$

The effective current I in the actuator coil is directly proportional to the torque constant k_m and inducing the torque

$$T_a = k_m I \tag{6}$$

by the BLDC motor. The voltage U is the system's input. The actuator current is obtained by

$$I = \frac{1}{R}\left(U - k_m \dot{\varphi}\right) \tag{7}$$

with the electrical resistance R and by neglecting the electrical inductance of the armature circuit.

The gear friction will be described by two different models. The first law fits very well to the catalog data wherat we will show in Sect. V that the second model can be very acurately fitted on our measurements.

One way of describing the friction term T_f of the gear, according to [10], is

$$T_f = -\text{sgn}\left(\dot{\varphi}\right)\left(T_{f,0} + \mu\left|T_l\right|\right) - \left(b + \gamma\left|T_l\right|\right)\dot{\varphi} \tag{8}$$

This is a classic approach with a static friction term ($T_{f,0}$), the Coulomb friction ($\mu\left|T_l\right|$), viscous friction ($b\dot{\varphi}$) and a coupled load and speed dependent term ($\gamma\left|T_l\right|\dot{\varphi}$). In the catalog of the gear manufacturer, experimental results on the efficiency η of the product are given for varying load, speed and temperature cases. During the design phase, this data can be used to compute the parameter $T_{f,0}$, μ, b and γ of (8), by solving the following constrained optimization problem [10]

$$\sum_i \left(\eta_{i,\text{catalog}} - \eta_{i,\text{model}}\right)^2 \rightarrow \min \tag{9}$$

$$T_{f,0} \geq 0, \quad \mu \geq 0, \quad b \geq 0 \tag{10}$$

The results of the parameter estimation of the investigated HarmonicDrive gears is described in Sect. VI. For another way to describe the friction, similar to HESS AND SOOM [11], we propose the following friction law

$$T_f = -\text{sgn}\left(\dot{\varphi}\right)\left(\bar{T}_{f,0} + \bar{\mu}\left|T_l\right|\right) - \bar{b}\dot{\varphi} - \frac{T_{f,S} - \bar{T}_{f,0}}{1 + \left(\frac{\dot{\varphi}}{\dot{\varphi}_S}\right)^2} \tag{11}$$

The first three terms have the same meaning as in (8). However, the bar indicates different values of these variables. The fraction term is describing the Stribeck Effect and is parameterized by $T_{f,S}$ and $\dot{\varphi}_S$.

IV. TESTBED AND EXPERIMENTS

In this section, the design of the testbed and the automatic test procedure is described. Furthermore, the investigated robotic drive modules are introduced.

A. Test Procedure

In our experiments, we aimed to identify the characteristic curve of the drive modules frictional behavior. Major influences on the friction are the velocity and the load torque[1]. Thus, in our experiments, measurements were conducted at the unbounded system with varying angular velocities and load torques. Considering a quasi-static state, and using the torque balance, according to (1) –(3), it is possible to directly calculate the friction torque, acting on the input side, based on the measurement of the load torque and the effective current

$$T_f = \frac{1}{N}T_l - k_m I \tag{12}$$

[1]The influence of temperature is not investigated in this study. All experiments were conducted after a warm-up phase. However, for an indication of the temperature, a temperature sensor was attached to the housing of the drive module.

The efficiency of the drive module is given by

$$\eta = \frac{T_l}{N\,k_m I} \tag{13}$$

This leads to a set of major system requirements on the testbed, which are described in the following section.

B. Requirements and Specifications

In order to fully characterize the drive modules, in particular to identify friction effects, it is necessary to measure the following quantities:

1) The torque T_a on the input side.
2) The position φ and velocity $\dot{\varphi}$ on the input side.
3) The load torque T_l on the output side.
4) The position q and velocity $\dot{q}$ on the output side.

Further requirements are:

5) It must be possible to change the load torque T_l in a close range from values close to zero up to the nominal torque of the most powerful investigated module.
6) It must be possible to reach the maximum velocity of the fastest module for any load case.
7) Experiments must be conducted without modifying the modules.
8) Modular design allows for testing of different drive modules.

The input torque cannot be measured directly, because it is not possible to access the motor or wave generator shaft without modifying the module. Thus, we rely on the measurement of the effective current I, measured by the motor controller and compute T_a with (6) using the torque constant provided by the motor manufacturer. The position and velocity of the input shaft can be measured with the incremental encoder of the modules.

C. Design of the Testbed

The maximum load torque for the design of the testbed is defined as the highest nominal torque of the investigated modules. To cover the complete range of possible load torques, we decided to use two mechanical configurations for the testbed. The first configuration covers lower load torques and the second configuration handles higher torques. Thus, we selected a torque sensor with two calibrated measuring ranges (i.e. $0-20\,\mathrm{Nm}$ and $20-200\,\mathrm{Nm}$) to ensure accurate results. To apply the load torque, we decided to use a current controlled hysteresis brake, due to the following advantages: the load torque is continuously adjustable, the brake torque is independent of the angular velocity, and due to the working principle, the brake torque is applied contact-free, thus the lowest possible load torque is only limited by the damping in the bearings. By definition, the brake torque always acts against the motion of the drive making it easy to control, in particular at reversing speeds. The brake is from the company Mobac and has a minimum torque of about $0.092\,\mathrm{Nm}$ and a maximum torque of $17\,\mathrm{Nm}$. In the first configuration the brake is directly connected to the torque sensor and in the second configuration, the brake is connected via a gear transmission to the torque sensor. The

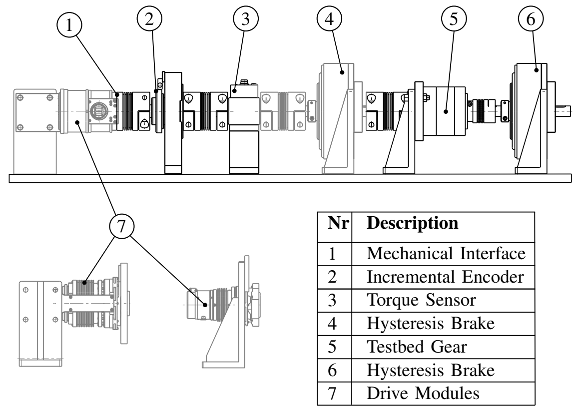

Fig. 3: Schematic overview of the testbed and its components.

components so far can be lined up on a testbed shaft, which is to be connected to the drive module‘s output shaft. To allow the required modularity of testing different modules a flange is provided. Combined with a grooved panel, as basis for the testbed, it is easy to design various adaptions, each suitable for a specific test module, respectively. Fig. 3 shows a side view of the designed testbed and its components. In the first configuration, the gear 5 and the brake 6 are decoupled with a clutch from the testbed. By the decoupling of the gear transmission, the back driving torque of the gear (i.e. the minimal required torque to move the gear from the slow side with no load on the faster side of the gear) is disconnected from the system. This allows the examination of very low load torques across speeds in different directions. To investigate higher load torques, the brake 4 can be removed and connected with the gear transmission 5 to the torque sensor. Furthermore, an incremental encoder is added to the testbed 2. The motor controller for the drives

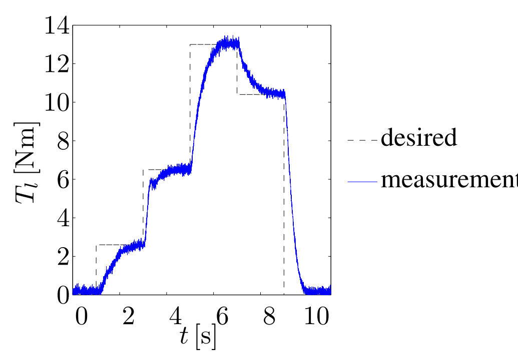

Fig. 4: Desired load torque on the testbed at $10\,\mathrm{rpm}$ without the testbed gear.

are from the company ELMO MOTION CONTROL and have a CAN bus communication interface. The brake torque is controlled using standard PI-feedback with an anti-wind up element, with voltage as manipulated variable and the torque sensor measurement as input. Fig. 4 shows the result of the brake control without the gear for desired torque step commands at a constant rotational velocity. The brake control is very stable for different velocities. The settling time of around $1\,\mathrm{s}$ is maintainable for the application. The data acquisition and the CAN bus communication is handled by a DSPACE board (ds1103). The software for the testbed is developed in MATLAB/SIMULINK. Tab. I summarizes the specifications of the major system components.

TABLE I: Major Specifications of the testbed components.

Component	Manufacturer (classification)	Specification
Incremental Encoder	ASM (PMIR5/PMIS4)	131072 ticks / rev.
Torque Sensor	Burster (8661-5200-V1202)	Meas. Range: 0-20 Nm 0-200 Nm
Brake	Mobac (HB-1750M-2DS)	Brake Torque: 0-15 Nm*
Gear	Neugart (PLE-120-5-OP01)	Ratio: 5

*Possible dissipation is 350 W continuously and 2400 W non continuously.

D. Experiments

The test bench, as presented in section IV-C, allows for testing over a broad range of angular velocities $\dot{\varphi}$ and loads T_l. For identification, a testing process to automatically and repeatably examine the modules was developed. The chosen approach was to set quasi-static points of operation, i.e. combinations of speed $\dot{\varphi}$ and load T_l. The points are equally spaced between maximum and minimum speeds and torques. An automatic mode, setting a constant speed and subsequently increasing the controlled load torque to a maximum value before moving to the next speed and repeating the process, was implemented. Each point is held for several seconds, to reach a quasi-static state. For the analysis of the data, the active current I and the load torque T_l are filtered by a low-pass filter after the experiment. Subsequently, the input torque T_a is calculated for each data point (cf. (6)) and friction as well as efficiency is determined via (12) and (13). As a last step, the mean values for each stationary point are calculated.

Two modules designed for the humanoid robot LOLA [12] (hip adduction and flexion, henceforth labeled A and B) and one test joint of the agricultural manipulator prototype (C) were experimentally investigated. Fig. 5 shows a picture of two out of the three investigated modules. In Tab. II a brief overview of the most important specifications is given.

TABLE II: Specifications of the investigated drive modules.

–	Units	A	B	C
Name	–	Lola Adduct.	Lola Flex.	Crops Test
k_m	Nm/A	0.13	0.097	0.075
Nominal Current	A	7	15	3.5
Gear model	–	HFUC-25-100	CSG-32-50	CSD-20-100

(a) Hip Adduction Joint (A)   (b) Test Joint (C)

Fig. 5: Robot Drive Modules

V. RESULTS

In this section, we present the main results of our experiments. In particular, the drive modules efficiency and the friction torque will be discussed. In Fig. 6 a picture of the testbed is shown.

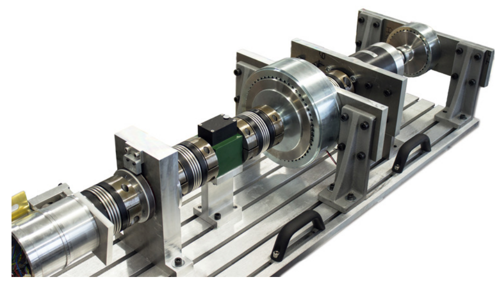

Fig. 6: Picture of the developed testbed.

Based on the measurements, the drive modules efficiency across the load torque is calculated and shown for several motor speeds in Fig. 7 (module A) and in Fig. 8 (module C). For reference, the efficiency of the modules gear transmission according to the catalog data is plotted as well. Especially for low velocities and high load torques, the efficiency measurements of the modules are below the catalog data. Since the

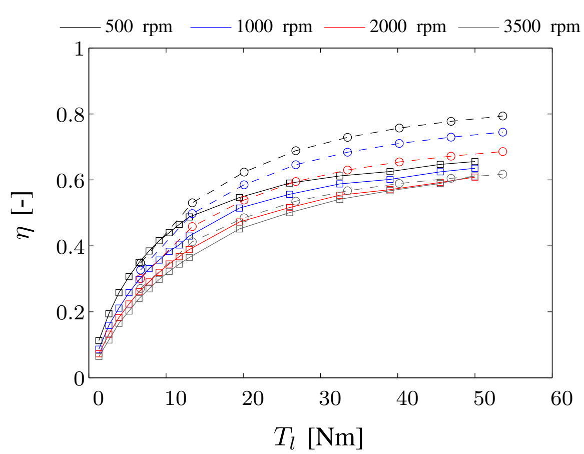

Fig. 7: The mean values of two efficiency measurements of the robot drive module A (–) compared with catalog data of the HarmonicDrive gear HFUC-25-100 (- -).

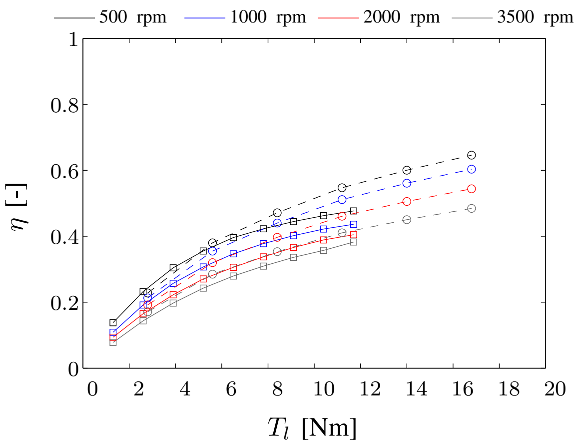

Fig. 8: The mean values of two efficiency measurements of the robot drive module C (–) compared with catalog data of the HarmonicDrive gear CSD-20-100 (- -).

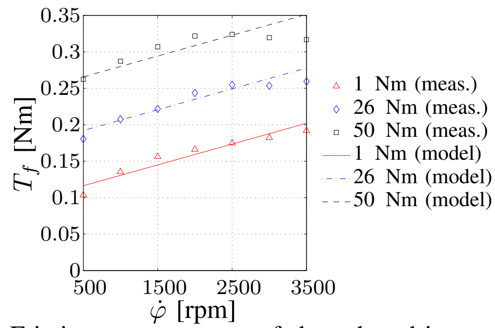

Fig. 9: Friction measurement of the robot drive module A among several load torques with a model fit of the friction law (8).

catalog data does not consider the friction loss in the motor shaft bearings, this seems to be a reasonable result. The friction law (8) is fitted to the measurements by solving (9) using the efficiency measurements instead of the catalog data. The friction torque T_f of module A and the fitted model is shown in Fig. 9. The estimated parameters of the friction law for all modules and the root-mean-square (RMS) of the fitting error are summarized in Tab. III. Note, that the coupled load and speed dependency $(\gamma\,|T_l|\,\dot{\varphi})$ is not represented in the curve fit of the measurements, i.e. $\gamma = 0$. Furthermore, the measurements indicate a nonlinear characteristic of the friction torque with respect to the motor angular velocity. The estimated parameters after the curve fit of (11) are given in Tab. IV and the model fit is shown in Fig. 10 for module A and in Fig. 11 for the module C. Comparing the curve fit of model (8) and (11) to the measurements in Fig. 9 and 10, the improved fit of model (11) is clearly visible. This is also reflected by comparing the RMS values in Tab. III and IV. The RMS value is reduced by the factor 2.4 for module A, 4.2 for module B and 2.1 for module C, clearly indicating the improved model fit of the friction law (11).

TABLE III: Parameter estimation result of the friction model (8) based on efficiency measurements.

–	A	B	C
$T_{f,0}$ $[Nm]$	0.098	0.456	0.067
μ $[-]$	3.10×10^{-3}	8.60×10^{-3}	4.4×10^{-3}
b $[Nm\,s/rad]$	2.73×10^{-4}	7.36×10^{-4}	2.26×10^{-4}
γ $[s/rad]$	0	0	0
RMS	1.11×10^{-2}	4.99×10^{-2}	6.4×10^{-3}

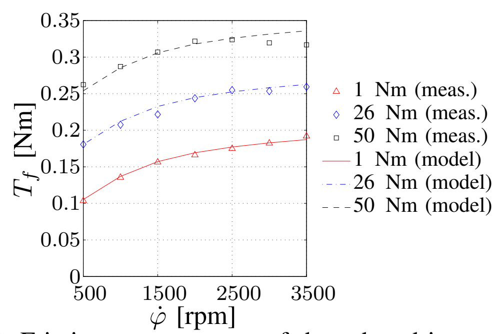

Fig. 10: Friction measurement of the robot drive module A among several load torques with a model fit of the friction law (11).

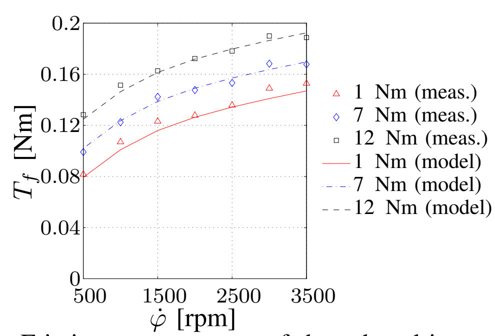

Fig. 11: Friction measurement of the robot drive module C among several load torques with a model fit of the friction law (11).

TABLE IV: Parameter estimation result of the friction model (11) based on efficiency measurements.

–	A	B	C
$\bar{T}_{f,0}$ $[Nm]$	0.174	0.479	0.112
$\bar{\mu}$ $[-]$	3.10×10^{-3}	1.20×10^{-2}	4.4×10^{-3}
$\bar{b}$ $[Nm\,s/rad]$	4.41×10^{-5}	4.275×10^{-4}	9.06×10^{-5}
$T_{f,s}$ $[Nm]$	0.079	0.078	0.057
$\dot{\varphi}_S$ $[rad/s]$	99.98	31.525	99.985
RMS	4.6×10^{-3}	1.20×10^{-2}	3.0×10^{-3}

VI. CONCLUSIONS

This paper presented the design of a modular testbed for experimental friction identification of robot drive modules. The identification allows for an improvement of our models, which is very important since we do not have joint torque sensors installed. In addition, an automatic test procedure to investigate and model steady-state friction effects has been described and implemented. Experiments have been conducted with three robotic drive modules with HarmonicDrive gear transmissions. All modules were developed at our institute. Although, the main source of friction is the gear transmission, the experiments showed that friction modeling based on measurements is significantly improved compared to modeling solely based on the catalog data of the gear's manufacturer.

In a next step, the test procedure, will be further improved. In particular, to obtain an accurate friction model for the complete operating range of the modules, lower velocities and load torques above the nominal motor torques will be investigated. To study the influence of temperature variations, another test procedure should be considered. Furthermore, all revolute joints of the CROPS manipulator prototype will be measured on the testbed. On the one hand, this verifies the design of the modules and on the other hand, we gain a very accurate dynamic model of the robot which can be further exploited by implementing a centralized control architecture.

APPENDIX

A. Harmonic Drive Efficiency based on Catalog Data

In Fig. 12 the efficiency of the Harmonic Drive gear transmission CSD-20-100 according to the catalog data is shown for several angular velocities of the wave generator and load torques on the gear output side at a temperature of 20 °C. In Tab. V the parameter estimates as a result of the curve fit according to (8) are shown.

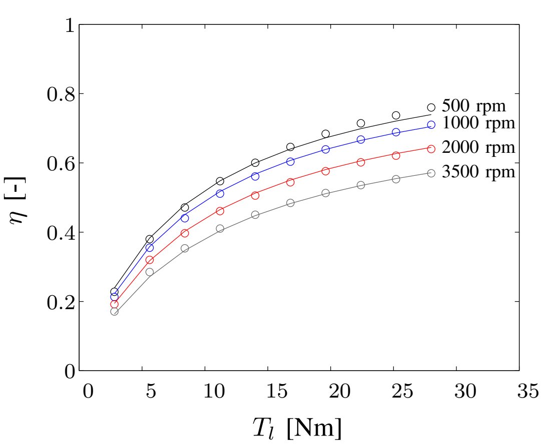

Fig. 12: Efficiency of the HarmonicDrive gear CSD-20-100 [13]. The plot shows the catalog data (○) and the corresponding curve fit (–) using (8).

TABLE V: Parameter estimation using the friction model (8) with a least squares fit of catalog data [13].

–	Gear HFUC-25-100	Gear CSG-32-50	Gear CSD-20-100
$T_{f,0}$ $[Nm]$	0.109	0.341	0.08
μ $[-]$	6.111×10^{-5}	1.2×10^{-3}	2.17×10^{-9}
b $[Nm\,s/rad]$	1.056×10^{-4}	2.035×10^{-4}	1.51×10^{-4}
γ $[s/rad]$	9.439×10^{-6}	1.244×10^{-5}	7.27×10^{-6}
RMS	8.6×10^{-3}	7.5×10^{-3}	7.5×10^{-3}

ACKNOWLEDGMENT

Special thanks go to G. Mayr, S. Gerer, P. Schneider, and G. Koenig for their technical support and contributions to the electrical and mechanical design.

REFERENCES

[1] T. Tuttle and W. Seering, "A nonlinear model of a harmonic drive gear transmission," *Robotics and Automation, IEEE Transactions on*, vol. 12, no. 3, pp. 368–374, 1996.

[2] A. Harnoy, B. Friedland, R. Semenock, H. Rachoor, and A. Aly, "Apparatus for empirical determination of dynamic friction," in *Proceedings of the American Control Conference*, vol. 1, 1994, pp. 546–550, cited By (since 1996):6. [Online]. Available: www.scopus.com

[3] A. Harnoy, B. Friedland, and S. Cohn, "Modeling and measuring friction effects," *Control Systems, IEEE*, vol. 28, no. 6, pp. 82–91, 2008.

[4] W. Seyfferth, A. J. Maghzal, and J. Angeles, "Nonlinear modeling and parameter identification of harmonic drive robotic transmissions," in *Robotics and Automation, 1995. Proceedings., 1995 IEEE International Conference on*, vol. 3, 1995, pp. 3027–3032 vol.3.

[5] H. Taghirad and P. Belanger, "An experimental study on modelling and identification of harmonic drive systems," in *Decision and Control, 1996., Proceedings of the 35th IEEE Conference on*, vol. 4, 1996, pp. 4725–4730 vol.4.

[6] H. D. Taghirad and P. R. Belanger, "Modeling and parameter identification of harmonic drive systems," *Journal of Dynamic Systems, Measurement, and Control*, vol. 120, no. 4, pp. 439–444, Dec. 1998. [Online]. Available: http://dx.doi.org/10.1115/1.2801484

[7] C. Kennedy and J. Desai, "Modeling and control of the mitsubishi pa-10 robot arm harmonic drive system," *Mechatronics, IEEE/ASME Transactions on*, vol. 10, no. 3, pp. 263–274, 2005.

[8] P. Hamon, M. Gautier, and P. Garrec, "Dynamic identification of robots with a dry friction model depending on load and velocity," in *Intelligent Robots and Systems (IROS), 2010 IEEE/RSJ International Conference on*, 2010, pp. 6187–6193.

[9] T. Tuttle, "Understanding and modeling the behavior of a harmonic drive gear transmission," Technical Report No. 1365, MIT, 1992. [Online]. Available: http://hdl.handle.net/1721.1/6803

[10] T. Buschmann, "Simulation and control of biped walking robots," PhD thesis, Technische Universität München, 2010.

[11] B. Armstrong-Hlouvry, P. Dupont, and C. C. D. Wit, "A survey of models, analysis tools and compensation methods for the control of machines with friction," *Automatica*, vol. 30, no. 7, pp. 1083 – 1138, 1994. [Online]. Available: http://www.sciencedirect.com/science/article/pii/0005109894902097

[12] S. Lohmeier, T. Buschmann, and H. Ulbrich, "Humanoid robot lola," in *Robotics and Automation, 2009. ICRA '09. IEEE International Conference on*, may 2009, pp. 775 –780.

[13] *General Catalog*, Harmonic Drive AG, Limburg/Lahn, 2011.